Polymer Nanotubules Obtained by Layer-by-Layer Deposition within AAO-Membrane Templates with Sub-100-nm Pore Diameters

*Younghyun Cho, Woo Lee, Young Kuk Jhon, Jan Genzer, and Kookheon Char**

The preparation and features of nanotubes consisting of various materials have attracted significant attention over the past few years because of their potential applications in microelectronics, biosensors, drug-delivery systems, and many other fields. The layer-by-layer (LbL) deposition technique on templates has been one of the most popular methods for the formation of nanotubes. Any size and shape of template can be utilized and the desired amount of various materials including polyelectrolytes,[1,2] biomolecules,[3,4] nanoparticles,[5,6] multiwalled nanotubes (MWNTs),[7] and quantum dots[8] can be readily incorporated within the thin-film geometry with nanoscale control through complementary interactions. Because the size and structural properties of materials thus prepared can be decided by the shapes of the templates used,[9–11] the morphological features of those materials can easily be tuned. More specifically, materials that possess extremely high aspect ratios can be achieved in large quantities based on the templates used. Consequently, many researchers have reported nanotube-fabrication processes based on the template-assisted LbL method.[12–20] In spite of these benefits, one of the hurdles of the method is associated with pore blockage generated from a polymer multilayer residing at the top surface of the template, which is most serious on relatively small pores. When porous substrates with diameters ≤400 nm are immersed in a polymer solution, polymer chains cannot diffuse readily into the pores and also cannot adsorb onto the inner-template walls due to the entropic entry barrier. The immediate consequence is that the pore mouth is covered and blocked by adsorbing polymers, impeding further migration and adsorption of polymer chains within the pores during the LbL process. Thus, the preparation of polymer nanotubes with small feature sizes has not been possible using the template-assisted LbL method employing nanostructured pores. In order to solve this problem, researchers have suggested various alternatives, such as the pressure-filter template technique, which can overcome the pore-blocking problem by applying external pressure,[16,18–20] mechanical removal of top polymer layers[12] at every deposition step, and selective chemical treatment[21] on the top surface. However, these techniques are time intensive, laborious, and quite costly. Furthermore, the inner surface of pores with diameter ≤200 nm cannot be uniformly coated, even if the techniques mentioned above are applied to the LbL templating method.

In this Communication, we report the successful preparation of well-defined polymeric nanotubules with diameter ≤100 nm through the template-assisted LbL method by controlling the ratio of the polymer dimension to the pore size, influencing the polymer diffusion in a narrow pore without the additional tedious steps mentioned above. In order to control the ratio of polymer dimension to pore size, we varied the molecular weight of adsorbing polymers, the chain conformation, and the aggregation condition by adjusting the valency of salts for strong polyelectrolytes as well as solution pH for weak polyelectrolytes. One advantage of our approach is that the exposed polymer multilayered surface of anodic aluminum oxide (AAO) substrates with pore diameter of 70 nm is about 20× larger than that having a pore diameter of 200 nm. This high surface-area-to-volume ratio could significantly improve the efficiency of various filtration-membrane applications.[12,22] The subsequent removal of AAO substrates leads to the preparation of nanotubular structures consisting of various materials (i.e., polymers, nanoparticles, and quantum dots) with extremely small sizes that have never been realized before.

Polymeric nanotubes were prepared by the LbL assembly within pores of AAO templates of ≈70 nm in diameter, as illustrated in **Scheme 1**. The AAO surfaces were first coated with 3-aminopropyl triethoxysilane (APTES). The positively charged APTES substrate would allow negatively charged polyelectrolytes to adsorb directly on the substrate. Subsequently, negatively charged polyelectrolytes,

Y. Cho, Prof. K. Char
Intelligent Hybrids Research Center
School of Chemical and Biological Engineering
The WCU Program of Chemical Convergence for Energy & Environment
Seoul National University
Seoul, 151-744, Korea
E-mail: khchar@plaza.snu.ac.kr
Dr. W. Lee
Korea Research Institute of Standards and Science (KRISS)
Daejon, 305-600, Korea
Dr. Y. K. Jhon, Prof. J. Genzer
Department of Chemical and Biomolecular Engineering
North Carolina State University
Raleigh, NC 27695-7905, USA
Dr. Y. K. Jhon
Division of Chemical Sciences
Army Research Office
Durham, NC 27703-9142, USA

DOI: 10.1002/smll.201001212

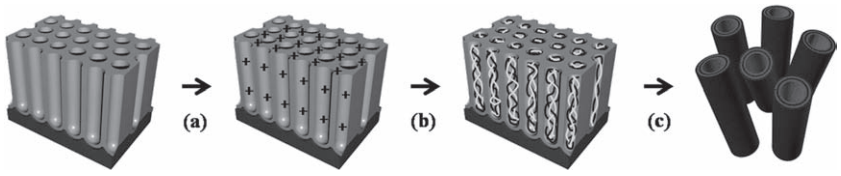

Scheme 1. A schematic depicting the preparation of LbL-assembled polymeric nanotubular structures formed within AAO templates: a) pretreatment of AAO templates with 3-aminopropyl triethoxysilane (3-APTES); b) LbL deposition of polyanionic and polycationic electrolytes within the AAO template; c) dissolution of the AAO template by either acid or base solution.

that is, poly(sulfonated styrene) (PSS) and poly(acrylic acid) (PAA), and positively charged polyelectrolytes, that is, poly(allylamine hydrochloride) (PAH), were alternatively assembled in aqueous solution by the dipping method until a desired number of bilayers was achieved. Subsequently, the nanotubes were separated by etching the AAO templates in either acidic or basic conditions.

In order to coat multilayer films uniformly on the entire nanocylindrical vertical sidewalls in the AAO without pore blockage, we add $CaCl_2$, a typical multivalent salt. The presence of a salt causes the polyelectrolyte chains to shrink due to the screening of electrostatic interactions between monomer units. When a monovalent salt is added to the polyelectrolyte solution, the charge of the polyelectrolyte chains is compensated because counter ions condense on the chains, thus diminishing the net polyelectrolyte charge. By adding multivalent salts, the charge of monomers associated with high-valency ions is reversed to the opposite charge. This behavior leads to electrostatic attraction between nonbonded monomers, which have their own charge, and oppositely charged monomers resulting from the association with counter ions. This effect, called ion bridging, allows for much-stronger polymer-chain contraction relative to simply adding the equivalent amount of monovalent-salt ions. If the amount of multivalent salt added is much higher than a certain level, the charge on the polyelectrolyte chains is fully neutralized and a total-net-charge inversion in an isolated polymer chain occurs and/or oppositely charged monomer units (due to collaboration with the multivalent salts) interact with nonbonded monomers with their own charge in adjacent polymer chains. This leads to the aggregation and precipitation of polyelectrolyte chains in aqueous polyelectrolyte solutions. This phenomenon has been explored theoretically,[23] in experiments,[24,25] and by computer simulations.[26,27]

Figure 1 shows field-emission scanning electron microscopy (FE-SEM) images (top view) of AAO pores filled with 15 bilayers of PSS and PAH multilayers as a function of $CaCl_2$ concentration. A decrease in pore size is shown in Figure 1a,b, and all the pores are blocked in Figure 1c,d. This indicates that the polyelectrolyte chains could diffuse and be adsorbed onto the inner surfaces without pore clogging caused by the entropic barrier under certain $CaCl_2$ concentration (Figure 1a,b). If the amount of $CaCl_2$ exceeds the critical concentration (>5 mM), the polyelectrolyte chains could form clusters that cover the top surface of the nanopores (Figure 1c,d). For the preparation of tubular structures, the adsorption behavior of polyelectrolyte chains also needs to be considered as well as the dimension issue. It has been well documented that the polyelectrolyte-multilayer thickness is approximately proportional to the salt concentration.[28–30] Even though the polymer dimension is small enough for migration into and adsorption onto the nanopores, if the thickness of multilayer films assembled in the interior of pores is overly thin due to a small amount of added salt and, concurrently, the adsorption density of polyelectrolyte chains is low resulting in low surface coverage due to strong interchain repulsions among polyelectrolyte chains, nanotubular structures can barely be formed by the LbL process (Figure 1a). We have observed that polymeric nanotubular structures can only be obtained with an optimum concentration of $CaCl_2$. However, with a monovalent salt, such as NaCl, the nanopore was clogged by polymer deposition at the top surface of the nanoporous substrates, regardless of the amount of NaCl added. In the present study, since the polymer nanotubules formed were thoroughly rinsed twice in pure water during the LbL deposition, we believe that excess amounts of both polyelectrolytes and salt ions, which are not directly associated with the polyelectrolyte chains in the multilayer

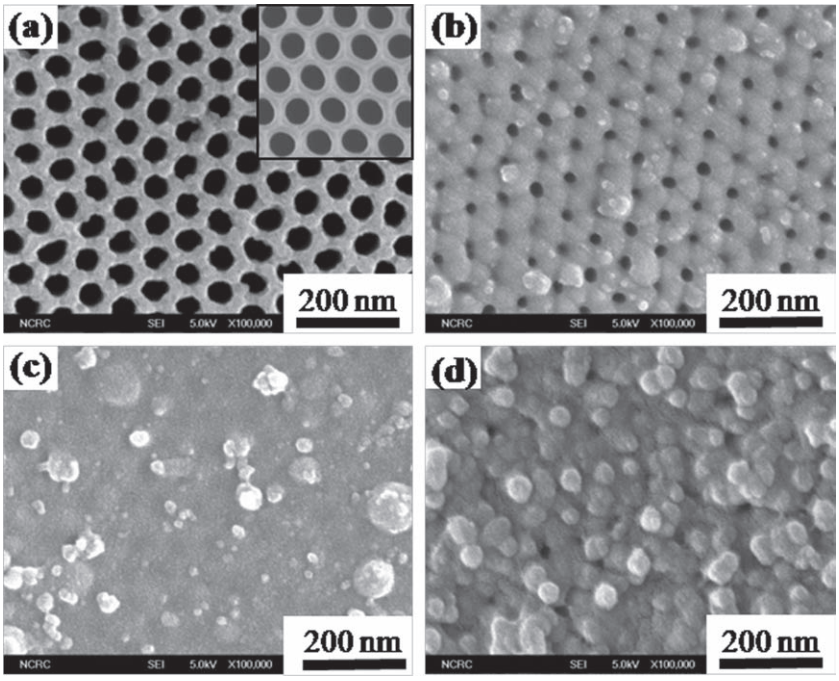

Figure 1. FE-SEM images of $(PSS/PAH)_{15}$ multilayers coated on the side walls of AAO templates as a function of $CaCl_2$ concentration: a) 1, b) 5, c) 50, and d) 100 mM. The inset of (a) shows the pristine AAO membrane (with a diameter of ≈70 nm) without polyelectrolyte deposition.

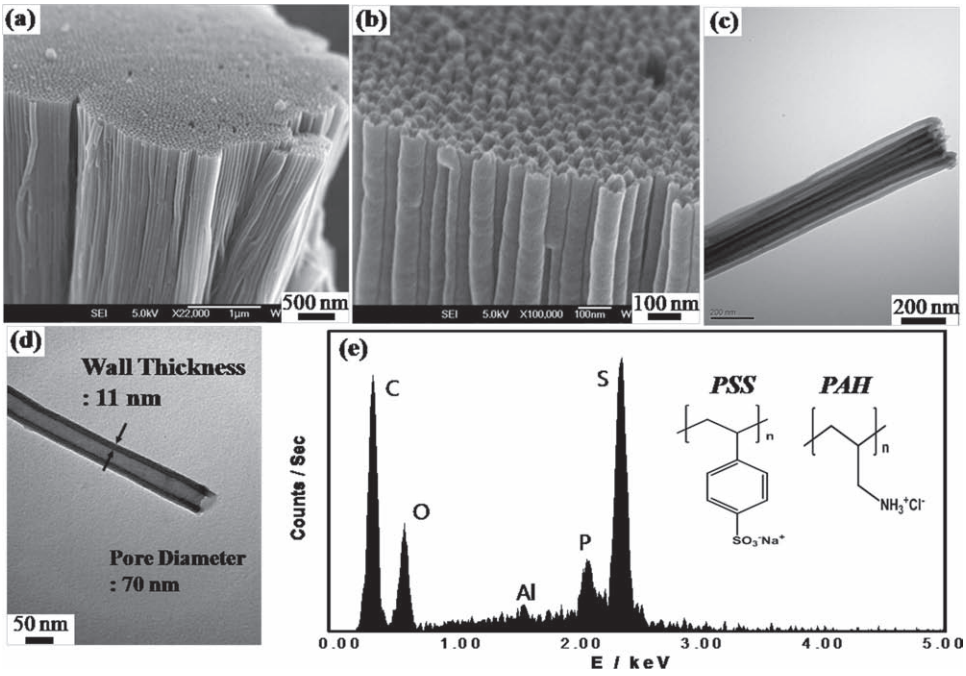

Figure 2. FE-SEM and TEM images and EDX spectrum of polymeric nanotubules (PNT) formed by $(PSS/PAH)_{15}$ multilayers in aqueous solution containing 5 mM $CaCl_2$ as a salt: a) low- and b) high-magnification SEM images of PNTs; c) low- and d) high-magnification TEM images of PNTs; e) EDX spectrum of PNTs.

structure, are completely removed. However, we still think that the salt ions directly associated with the polyelectrolyte chains would remain in the polymeric nanotubules even after the thorough rinsing of the films.

Dynamic light scattering (DLS) measurements give an insight into why an optimum concentration of multivalent salt is likely to be the crucial factor for the formation of uniform adsorption of polyelectrolytes within narrow pores (see Figure S1 in the Supporting Information (SI)). The DLS results show that the polymer dimension of PSS is minimized by adding 5 mM of divalent salts that cause the ion-bridging effect. In the same manner, the dimension of PAH in aqueous solution has the lowest value at a concentration of of $CaCl_2$ of 5 mM.

Figure 2a,b shows low- and high-magnification FE-SEM images, respectively, of multilayered polymer nanotubes consisting of fifteen PSS/PAH layers after the removal of a AAO template by wet chemical etching. The polymer layer deposited at the top surface of the template was eliminated by oxygen-plasma etching prior to the dissolution of AAO templates to yield individual nanotubes. The outer diameter of the nanotubes obtained was found to be ≈70 nm and the length was ≈70 μm; the nanotubes thus prepared were similar in size to the pore diameter as well as to the pore length of the AAO substrate. Figure 2c,d shows transmission electron microscopy (TEM) images of bundles of nanotubes, as well as a single nanotube, respectively, proving that the nanotubes have an inner-void diameter of ≈48 nm with a uniform wall thickness of 11 nm, as prepared from 15 bilayers of PSS/PAH. The wall thickness of the nanotubes could be finely controlled by the number of bilayers through the LbL deposition process. Moreover, the composition of the nanotubes is further confirmed by energy-dispersive X-ray spectroscopy (EDX), as shown in Figure 2e. The presence of sulfur in the spectrum demonstrates that PSS polyelectrolyte chains are successfully incorporated into the polymer nanotubes.

Another approach aimed at the preparation of polymeric nanotubes with small feature sizes involves the adjustment of pH in weak polyelectrolyte solutions. Weak polyelectrolytes with relatively low molecular weights (PAA: 1.8 kDa and PAH: 15 kDa) were employed for the LbL process because pore clogging was always observed with polyelectrolytes with relatively high molecular weights (PAA: 100 kDa and PAH: 70 kDa), regardless of pH adjustment. It is well known that the pH of weak polyelectrolyte solutions crucially influences the charge density of polyelectrolyte chains.[31–33] This, in turn, has a strong effect on the variation of polymer-chain conformations as well as the aggregation state of polymer chains due to variation of the degree of ionization.[34,35] By simply adjusting the solution pH, it is possible to tailor the thickness of the multilayer film[2] by varying the polymer-chain dimension. Moreover, solution pH plays an important role in polymer diffusion in narrow pores and the adsorption during the LbL process. **Figure 3** shows FE-SEM images (top view) of pores with 15 bilayers of PAA and PAH prepared at various pH combinations ($K = x/y$, where x and y are the pH of PAA and PAH solutions, respectively). The decrease in pore diameter due to adsorbed polymer multilayers was observed with $K = 4/3$ and 4/2 combinations. No pore blocking was observed up to 15 bilayers (Figure 3c,d). In contrast, all the pores were completely clogged by the polymer layers adsorbed near the pore mouths with $K = 6/6$ and 5/4 combinations (Figure 3a,b). While pristine pores were observed under the cracked polymer layer at $K = 6/6$ (inset in Figure 3a), at $K = 5/4$, a

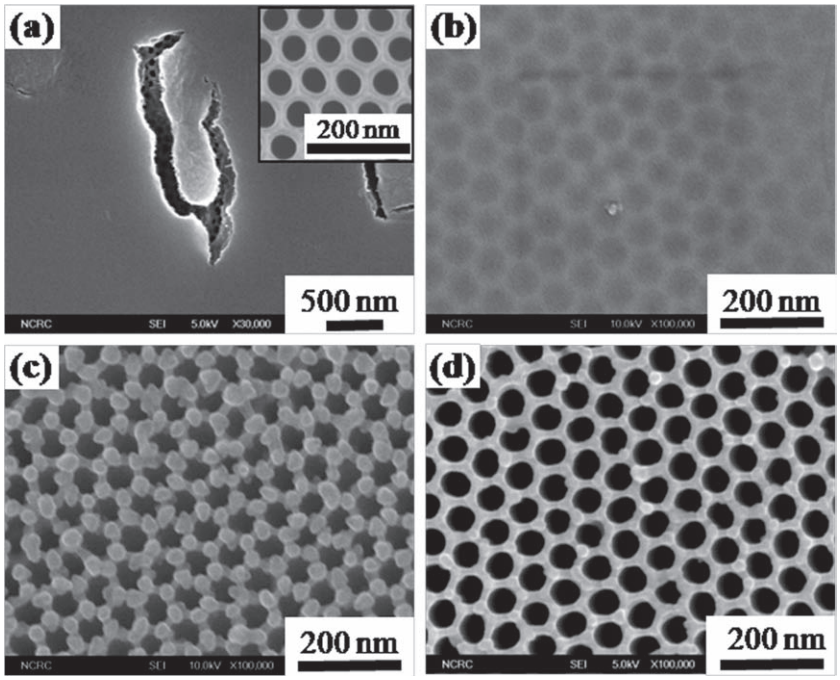

Figure 3. FE-SEM images of $(PAA/PAH)_{15}$ multilayers coated on the side walls of AAO templates as a function of pH deposition condition ($K = x/y$, where x and y are the pH of PAA and PAH solutions, respectively): a) $K = 6/6$; b) $K = 5/4$; c) $K = 4/3$; d) $K = 4/2$. The inset of (a) shows the pristine AAO membrane (with a diameter of ≈70 nm) before polyelectrolyte deposition.

relatively thin polymer layer covers the pores of the AAO substrate (Figure 3b). As will be further demonstrated below, this clogging results from the large polymer dimension of each polyelectrolyte chain (either PAA or PAH) relative to the size of pores, as well as the thick bilayer thickness observed at these pH conditions. Therefore, at $K = 6/6$, a polymer multilayer forms at the top of the AAO substrates instead of the inner side walls of pores. Interestingly, in the case of $K = 4/2$, the amount of adsorbed polymers on the AAO surface was low compared to that with $K = 4/3$. As mentioned above, in order to obtain the desired polymeric nanotubes, the adsorption behavior of polyelectrolyte chains within the pores must also be considered as well as the dimension issue. The lack of adsorbed polymers during the LbL deposition with $K = 4/2$ resulted in incomplete polymer nanotubes; broken nanotubes with many defects were observed after removing the AAO substrate. These results thus indicate that, among the cases studied in the present work, the $K = 4/3$ combination provided the optimal conditions for obtaining polymer nanotubes, although the polymer dimension at the $K = 4/2$ combination was also relevant to let the polyelectrolyte chains diffuse into narrow pores.

The thickness of multilayer films of weak polyelectrolytes on flat silicon substrates grows with increasing the number of bilayers under the same experimental conditions as used for realizing polymer multilayers within the pores (**Figure 4**). The Rubner group demonstrated that dramatic changes in the thickness of sequentially adsorbed polyelectrolyte layers can be achieved with a small change in solution pH.[2] Ellipsometric data clearly show that the thickness of multilayer films at combinations of $K = 6/6$ and 5/4 was much larger than that at $K = 4/3$. This variation in bilayer thickness on flat surfaces gives an insight into why pore blocking was observed at either $K = 6/6$ or 5/4 combinations and why the polymeric nanotubules prepared from porous structures at a combination of $K = 4/2$ do not have sufficient mechanical strength. Consequently, it is concluded that the nanopores can be uniformly coated only under the optimal polymer solution condition, which provides conditions for the relevant polymer diffusion inside the pores and subsequent build-up of multilayers due to adsorption. In the case of polymer multilayers formed within the pores, we assume that the composition of polymeric nanotubules would not be grossly different from the composition of multilayers prepared on flat substrates because the multilayer growth behavior on flat substrates, as shown in Figure 4, qualitatively shows a similar trend for the pore-blocking behavior at different pH combinations.

DLS was also employed to obtain information about the polymer conformation under various pH solution conditions. The chain dimension of PAH was low under relatively low pH conditions (pH = 2 and pH = 3) compared with the cases for pH = 4 and pH = 6 (see Figure S2 in the SI). Moreover, the chain dimension of PAA was reduced under relatively low pH condition (pH = 4). These DLS data strongly support the notion that the uniform deposition of multilayers inside the pore is only possible within a limited pH range.

FE-SEM and TEM images of polymer nanotubes consisting of weak polyelectrolytes $(PAA/PAH)_{15}$ assembled at a combination $K = 4/3$ after the removal of the AAO

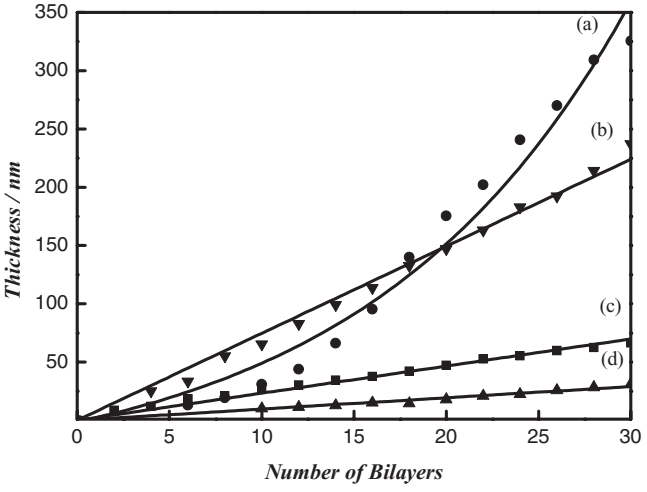

Figure 4. The growth curve of $(PAA/PAH)_n$ multilayer films on flat substrates deposited in various pH combinations ($K = x/y$, where x and y are the pH of PAA and PAH solutions, respectively): a) $K = 6/6$; b) $K = 5/4$; c) $K = 4/3$; d) $K = 4/2$.

small NANO MICRO

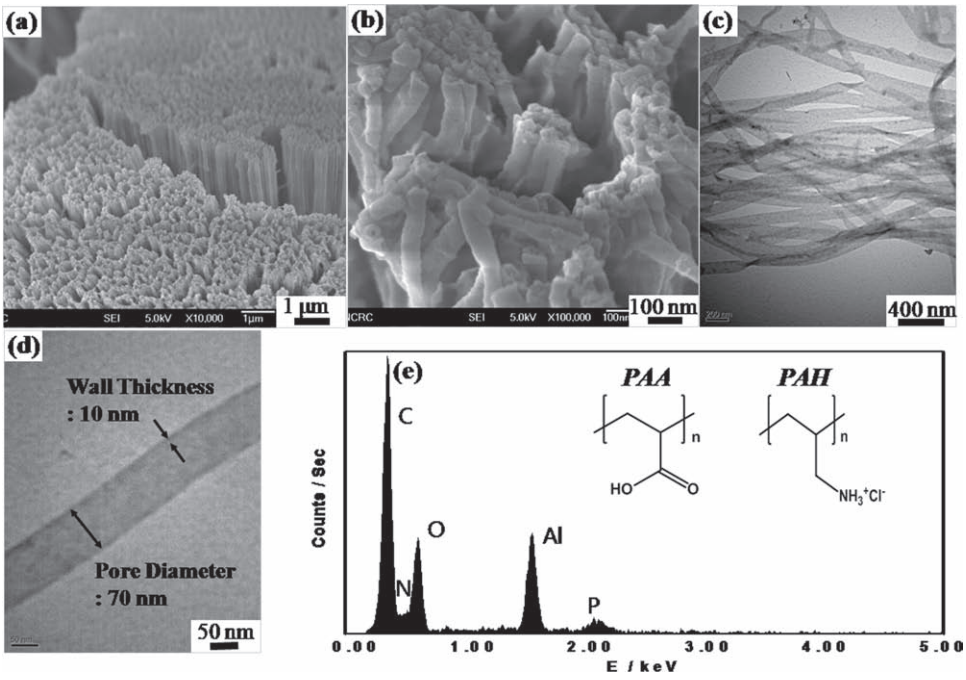

Figure 5. FE-SEM and TEM images and EDX spectrum of polymeric nanotubules (PNTs) of crosslinked $(PAA/PAH)_{15}$ multilayers prepared by the sequential deposition of PAA and PAH ($K = 4/3$): a) low- and b) high-magnification SEM images of PNTs; c) low- and d) high-magnification TEM images of PNTs; e) EDX spectrum of PNTs.

template are shown in **Figure 5**. Since the assembled multilayer structures were damaged and sometimes decomposed in the harsh acidic or basic condition during the liberation of polymeric nanotubular structures from the template, we crosslinked the PAA/PAH multilayered structures by heat treatment at 180 °C for 24 h to form amide bonds between polyelectrolyte chains prior to the dissolution of the AAO template. Under those treatment conditions, the crosslinked polymeric structures appear to be quite stable in a wide range of pH conditions.[36] The EDX characterization of the samples shows a strong oxide peak originating from PAA, a weak nitrogen peak from PAH, and a characteristic carbon peak from both PAA and PAH. The wall thickness obtained from the TEM images was ≈10 nm and the diameter of the nanotube was approximately ≈70 nm, corresponding to the pore size of AAO templates used in this experiment. Interestingly, the wall thickness was much thinner than that of the corresponding multilayer film prepared on flat substrates under the same experimental conditions. Our results contrast with previous reports that the thickness of multilayer films in confined geometries is larger than that on flat substrates. In these previous studies, researchers attribute this difference in bilayer thickness within the pores to incomplete drainage of the solutions during the LbL process,[14] stronger polymer adsorption due to the curvature of a pore,[16] or entanglement of polyelectrolyte chains in the confined geometry.[19] We believe our contrary result arose from the small pore size (70 nm in diameter) used in our experiments. When a porous structure is immersed in a polymer solution, solvent molecules penetrate the pore channels. At the same time, some polymer chains diffuse into the pore channels. Eventually, the solution in the interior of the porous channel achieves a equilibrium concentration state with the exterior solution. The ratio of the interior polymer concentration c_I to the exterior concentration c_E is called the partition coefficient (Equation 1).

$$K = C_I / C_E. \tag{1}$$

When a solution containing an ideal chain is in contact with the porous channel, this partition coefficient, K, is expressed as Equation 2,

$$\ln K \sim -N(a/d_p)^2, \tag{2}$$

where N, a, and d_p represent the number of monomers, monomer size, and pore diameter, respectively.[37,38]

Therefore, the number of polymers migrating into the pore exponentially increases with the pore diameter. When the pore diameter is large enough or if additional techniques, such as a pressure-filter template method, are applied to force the polymers inside the pores, the number of polymer chains that can be diffused into the larger pores is not much different from that on the flat surface, resulting in a thicker multilayer film due to the reasons mentioned above. However, in an extremely narrow pore, as investigated in the present case, the number of polymer chains penetrating into the pores is significantly reduced due to the entropic barrier, yielding a thinner multilayer compared to the situation involving polymer diffusion and adsorption in larger pores or on flat substrates.

In summary, we have demonstrated the preparation of polymeric nanotubules with very small feature sizes based

on the template-assisted LbL method by adjusting the ratio of polymer dimension to pore size. Using this approach, it is possible to prevent polymer deposition onto the pore mouths, which obstruct the formation of multilayered nanotubes within narrow pores, by simply manipulating the deposition condition of polyelectrolyte solutions. Moreover, it is anticipated that our investigations can be extended to the incorporation of various functional materials, such as quantum dots, nanoparticles, and biomolecules, into these well defined small polymeric nanostructures for specific applications ranging from biosensors and catalytic membranes to electronics, allowing their performance to be greatly enhanced.

Experimental Section

Preparation of AAO Membrane: Nanoporous AAO templates were synthesized by the two-step anodization method.[39] First, high-purity aluminum plates (99.999%) were degreased in acetone then electropolished in 1:3 volume mixtures of perchloric acid and ethanol by a constant voltage of 20 V for 5 min. The first anodization was performed under constant voltage of 40 V for ≈5–10 h in oxalic acid solution (0.3 M) at 15 °C. Afterwards, the porous oxide layer was chemically removed by an aqueous mixture of chromic acid (1.8 wt%) and phosphoric acid (6 wt%) for ≈10–15 h at 45 °C. Subsequently, pretextured aluminum plates were anodized under the same experimental conditions as used for the first anodization step for 24 h.

Preparation of Multilayered Polymeric Nanotubules: PSS (M_w = 70 000), PAA (M_w = 1800), and PAH (M_w = 15 000) were purchased from Sigma-Aldrich and used as received. Anionic and cationic polyelectrolytes were alternatively deposited onto an APTES-treated AAO template by using an automated slide stainer. Polyelectrolyte multilayers were assembled by dipping into polyanion solution and polycation solution (1 mg mL^{-1} for 30 min each). After the deposition of each polyelectrolyte layer, the sample was thoroughly rinsed in two baths of Milli-Q water for 5 min each. The assembled polymeric nanotubules were released from the AAO template by dissolving aluminum oxide in phosphoric acid aqueous solution at 45 °C for 1 h.

Characterization: TEM measurements were carried out using a JEOL JEM1010 operating at 100 kV. TEM samples were prepared by placing a few drops of sample suspension onto copper grids. The surface morphology and EDX measurements were investigated using a JEOL JSM-6701F. The thicknesses of multilayer films on flat silicon substrates were measured by ellipsometry (Gaertner Scientific Corp.). For DLS measurements, a 532-nm solid-state laser (Crystalaser, Reno, NV) was used as the light source. Scattered light intensities were measured at 90° from the light source. All the polyelectrolyte solutions were filtered through a 0.2-μm Millex polytetrafluoroethylene syringe filter.

Supporting Information

Supporting Information is available from the Wiley Online Library or from the author.

Acknowledgements

This work was financially supported by the National Research Foundation of Korea (NRF) Grant funded by the Korean Ministry of Education, Science and Technology (MEST) (The Creative Research Initiative Program (No. 2010–0018290), NANO Systems Institute-National Core Research Center (No. R15–2003-032–05001-0),The WCU Program of C2E2 (R31–10013) and graduate programs at Seoul National University through the BK 21 Program. We also acknowledge the financial support from the Korean Ministry of Knowledge Economy (MKE) on SystemIC2010 Project. We are also grateful to Dr. Laura Beth Dong and Prof. Geroge Roberts for DLS measurements.

[1] G. Decher, *Science* **1997**, *277*, 1232.
[2] S. S. Shiratori, M. F. Rubner, *Macromolecules* **2000**, *33*, 4213.
[3] P. J. Yoo, K. T. Nam, J. F. Qi, S. K. Lee, J. Park, A. M. Belcher, P. T. Hammond, *Nat. Mater.* **2006**, *5*, 234.
[4] Z. Y. Tang, Y. Wang, P. Podsiadlo, N. A. Kotov, *Adv. Mater.* **2006**, *18*, 3203.
[5] F. Caruso, R. A. Caruso, H. Mohwald, *Science* **1998**, *282*, 1111.
[6] D. Lee, M. F. Rubner, R. E. Cohen, *Nano Lett.* **2006**, *6*, 2305.
[7] S. W. Lee, B. S. Kim, S. Chen, Y. Shao-Horn, P. T. Hammond, *J. Am. Chem. Soc.* **2009**, *131*, 671.
[8] M. Hojeij, B. Su, S. X. Tan, G. Meriguet, H. H. Girault, *ACS Nano* **2008**, *2*, 984.
[9] K. H. A. Lau, H. Duran, W. Knoll, *J. Phys. Chem. B* **2009**, *113*, 3179.
[10] J. Xu, J. Xia, J. Wang, J. Shinar, Z. Lin, *Appl. Phys. Lett.* **2006**, *89*, 133110.
[11] P. Molian, Z. Lin, Q. Zou, *J. Nanosci. Nanotechnol.* **2008**, *8*, 2163.
[12] D. M. Dotzauer, J. H. Dai, L. Sun, M. L. Bruening, *Nano Lett.* **2006**, *6*, 2268.
[13] Z. J. Liang, A. S. Susha, A. M. Yu, F. Caruso, *Adv. Mater.* **2003**, *15*, 1849.
[14] D. Lee, A. J. Nolte, A. L. Kunz, M. F. Rubner, R. E. Cohen, *J. Am. Chem. Soc.* **2006**, *128*, 8521.
[15] D. Lee, R. E. Cohen, M. F. Rubner, *Langmuir* **2007**, *23*, 123.
[16] S. F. Ai, G. Lu, Q. He, J. B. Li, *J. Am. Chem. Soc.* **2003**, *125*, 11140.
[17] C. L. Feng, X. H. Zhong, M. Steinhart, A. M. Caminade, J. P. Majoral, W. Knoll, *Adv. Mater.* **2007**, *19*, 1933.
[18] Y. Tian, Q. He, C. Tao, J. B. Li, *Langmuir* **2006**, *22*, 360.
[19] H. Alem, F. Blondeau, K. Glinel, S. Demoustier-Champagne, A. M. Jonas, *Macromolecules* **2007**, *40*, 3366.
[20] M. L. Bruening, D. M. Dotzauer, P. Jain, L. Ouyang, G. L. Baker, *Langmuir* **2008**, *24*, 7663.
[21] S. F. Hou, C. C. Harrell, L. Trofin, P. Kohli, C. R. Martin, *J. Am. Chem. Soc.* **2004**, *126*, 5674.
[22] S. B. Lee, D. T. Mitchell, L. Trofin, T. K. Nevanen, H. Soderlund, C. R. Martin, *Science* **2002**, *296*, 2198.
[23] F. J. Solis, M. O. de la Cruz, *J. Chem. Phys.* **2000**, *112*, 2030.
[24] K. Besteman, K. Van Eijk, S. G. Lemay, *Nat. Phys.* **2007**, *3*, 641.
[25] Y. Murayama, Y. Sakamaki, M. Sano, *Phys. Rev. Lett.* **2003**, *90*, 018102.
[26] P. Y. Hsiao, E. Luijten, *Phys. Rev. Lett.* **2006**, *97*, 148301.
[27] S. Liu, K. Ghosh, M. Muthukumar, *J. Chem. Phys.* **2003**, *119*, 1813.
[28] S. T. Dubas, J. B. Schlenoff, *Macromolecules* **1999**, *32*, 8153.
[29] S. T. Dubas, J. B. Schlenoff, *Macromolecules* **2001**, *34*, 3736.
[30] H. W. Jomma, J. B. Schlenoff, *Macromolecules* **2005**, *38*, 8473.

[31] J. Cho, J. Hong, K. Char, F. Caruso, *J. Am. Chem. Soc.* **2006**, *128*, 9935.
[32] T. C. Wang, M. F. Rubner, R. E. Cohen, *Langmuir* **2002**, *18*, 3370.
[33] J. Choi, M. F. Rubner, *Macromolecules* **2005**, *38*, 116.
[34] M. Sedlak, *J. Chem. Phys.* **2002**, *116*, 5256.
[35] J. Park, Y. W. Choi, K. Kim, H. Chung, D. Sohn, *Bull. Korean Chem. Soc.* **2008**, *29*, 104.
[36] F. Mallwitz, A. Laschewsky, *Adv. Mater.* **2005**, *17*, 1296.
[37] P. G. d. Gennes, *Scaling Concepts in Polymer Physics*, Cornell University Press, Ithaca, New York **1979**, pp. 324.
[38] A. I. U. Grosberg, A. R. Khokhlov, *Statistical Physics of Macromolecules*, AIP Press, New York **1994**, pp. xxvii, 350.
[39] H. Masuda, K. Fukuda, *Science* **1995**, *268*, 1466.

Received: July 17, 2010
Revised: August 2, 2010
Published online: November 11, 2010

